Exact quantization condition for anharmonic oscillators (in one dimension)

1994 J. Phys. A: Math. Gen. 27 4653

(http://iopscience.iop.org/0305-4470/27/13/038)

J. Phys. A: Math. Gen. 27 (1994) 4653–4661. Printed in the UK

Exact quantization condition for anharmonic oscillators (in one dimension)

André Voros

CEA, Service de Physique Théorique†, Centre d'Etudes de Saclay, F–91191 Gif-sur-Yvette Cedex, France

Received 14 March 1994

Abstract. An exact quantization condition is given for the one-dimensional Schrödinger operator with a homogeneous anharmonic potential q^{2M}. It has the form of an explicit mapping from level sequences to level sequences, involving a Bohr–Sommerfeld-like quantization step, and having the exact spectrum as fixed point. Numerical tests and an approximate linear theory both suggest, at least for the few lowest M, that the mapping has a contractive region: when an initial level sequence is only asymptotically correct to lowest order, its iterates are seen to converge term by term towards the exact eigenvalues. This type of approach ought to extend to general polynomial potentials.

1. The Bohr–Sommerfeld quantization scheme

We are interested in the quantization mechanism which fixes the eigenvalues of a one-dimensional Schrödinger operator $-\hbar^2 d^2/dq^2 + V(q)$ when the potential $V(q)$ is polynomial [1] and confining (i.e. bounded below). The energy levels are then purely discrete, their sequence grows to $+\infty$ and they satisfy, to a very good approximation, the Bohr–Sommerfeld quantization rule

$$\oint p_E \, dq = S(E) = 2\pi(k + \tfrac{1}{2})\hbar \qquad k \text{ integer} \tag{1.1}$$

which is exact for harmonic oscillators; for any other V (of degree $2M > 2$) the formula is only asymptotic as $k \to +\infty$ and, moreover, the higher-order correction terms (in powers of $\hbar$) always build up divergent series which cannot be resummed. The divergence tells us that the usual semiclassical expansion fails to capture the exact structure of the spectrum quantization in general.

We will discuss alternative eigenvalue conditions which are exact and use the Bohr–Sommerfeld quantization mechanism. We mean by the latter (assuming a single-well potential for simplicity) that a reparametrization $\Sigma(E)$ of the $\{E \geqslant \min V\}$ half-line is defined through $d\Sigma(E) = \Theta(E)\,dE$ where $\Theta(E)$ is some measure density and that the new arclength values $\Sigma(E)$ are quantized as $ak + b$, k integer; accordingly, a spectral staircase function $\mathcal{N}(E)$ arises from the smooth function $\Sigma(E)$, a process to be called a BS mapping. For instance, the semiclassical quantization (1.1) uses for $\Theta(E)$ the period $T(E)$ of the

† Laboratoire de la Direction des Sciences de la Matière du Commissariat à l'Energie Atomique.

0305-4470/94/134653+09$19.50

classical trajectory $\{p^2 + V(q) = E\}$, hence for $\Sigma(E)$ the classical action $S(E)$; the BS mapping is $\mathcal{N}(E) = \mathcal{Q}\{S\}(E)$, where

$$\mathcal{Q}\{\Sigma\}(E) = \sum_k \theta(\Sigma(E) - (2k+1)\pi\hbar) \tag{1.2}$$

and θ is the Heaviside step function. The Poisson summation formula re-expresses this as

$$\mathcal{Q}\{\Sigma\} = \frac{1}{2\pi\hbar}\Sigma + \frac{\mathrm{i}}{2\pi}\sum_{m\neq 0}\frac{(-1)^m}{m}\mathrm{e}^{-\mathrm{i}m\Sigma/\hbar} = \overline{\mathcal{Q}}\{\Sigma\} + \mathcal{Q}_{\mathrm{osc}}\{\Sigma\} \qquad \left(\overline{\mathcal{Q}}\{\Sigma\} = \frac{1}{2\pi\hbar}\Sigma\right). \tag{1.3}$$

In the classical limit, where the density of states becomes continuous, $\mathcal{Q}$ ($\sim \overline{\mathcal{Q}}$) is a linear map but very much not in the quantum regime! (Hence overturning the cliché 'classical = nonlinear, quantum = linear'.)

2. Results (homogeneous potentials)

Our current results basically refer to the monomial potential $V(q) = q^{2M}$, that is easier to handle due to its high degree of symmetry. (The dependence of all quantities upon the parameter M will be understood.)

Besides the semiclassical rule (1.1), a fully $\hbar$-expanded form is available term by term; by a scaling property, it is a power series of a single variable [2]:

$$\Sigma^0(\hbar^{-2M/(M+1)}E) = \sum_{n=0}^{+\infty} b_n \left(\frac{E^{(M+1)/2M}}{\hbar}\right)^{1-2n}$$
$$= 2\pi(k+\tfrac{1}{2}) \qquad (\text{with } S(E) \equiv b_0 E^{(M+1)/2M}) \tag{2.1}$$

which allows us to set $\hbar = 1$. The (formal) expression $\Sigma^0(E)$, now asymptotic for $E \to +\infty$, is a factorially divergent series [3], except for $M = 1$ (harmonic oscillator) where it reduces to its leading term $S(E) = \pi E$.

2.1. The exact Bohr–Sommerfeld conditions

Our main result is that we have identified exact resummations of the quantization condition (2.1) in a form that is valid for arbitrary M (except, interestingly, $M = 1$ for which our construction breaks down). In fact, we have heavily resorted to parity symmetry to simplify the analysis and have obtained distinct exact quantization conditions for the even and odd spectra as

$$\Sigma_+(E) = 2\pi(k + \tfrac{1}{2} + C_M) \qquad k \text{ even} \tag{2.2+}$$
$$\Sigma_-(E) = 2\pi(k + \tfrac{1}{2} - C_M) \qquad k \text{ odd} \tag{2.2−}$$
$$C_M = \frac{M-1}{2(M+1)}.$$

For any $M > 1$ these arclengths $\Sigma_\pm(E)$ are exactly the field fluxes through the interval $[0, E]$ of certain charge distributions in the complex E-plane (in the sense of 2D electrostatics in a real plane). These distributions have a quantum-dynamical content, just as the semiclassical arclength $S(E)$ had a classical one.

Specifically, the charge distribution which generates either quantization condition (2.2±) for $V(q) = q^{2M}$ is the corresponding (even or odd) spectrum itself simply rotated by the angle $2\pi/(M+1)$, and carrying a charge $+4$ at each site (or, more symmetrically, charges $+2$ there and -2 at the complex conjugate locus). Equivalently, the arclength functions are given by the convergent sums

$$\Sigma_{\pm}(E) = 4 \sum_{\substack{\ell \\ \text{even} \\ \text{odd}}} \theta_{E_\ell}[0, E] \qquad \theta_{E_\ell}[0, E] = \operatorname{Arctan} \frac{\sin(2\pi/(M+1))\, E}{E_\ell - \cos(2\pi/(M+1))\, E} \in (0, \pi) \tag{2.3}$$

where $\theta_{E'}[E'', E]$ stands for the angular width of the interval $[E'', E]$ as seen from the point $e^{2\pi i/(M+1)}E'$. The resulting functions $\Sigma_{\pm}(E)$ and densities $\Theta_{\pm}(E)$ are shown in figure 1 for the quartic case ($M = 2$).

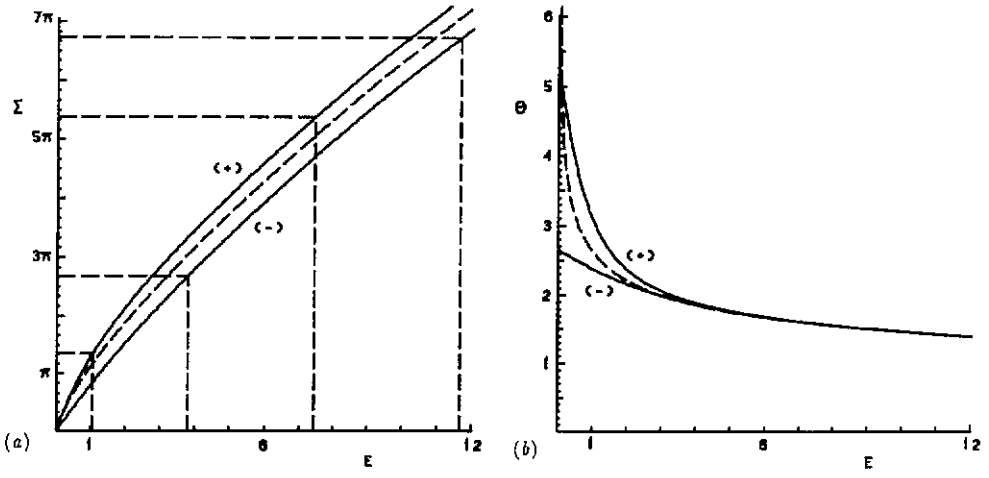

Figure 1. Quantization of the quartic ($M = 2$) potential q^4: (+), even-parity curves; (−), odd-parity curves; broken curves, semiclassical curves. (*a*) The arclength functions $\Sigma_{\pm}(E)$ against the action $S(E) = b_0 E^{3/4}$ (broken), with $b_0 = (2/\pi)^{1/2}\Gamma(1/4)^2/3$ and $\lim_{E\to+\infty}(\Sigma_{\pm}(E) - S(E)) = \pm\pi/3$; the exact quantization of the lowest four levels is depicted. (*b*) The flux densities $\Theta_{\pm}(E) = \mathrm{d}\Sigma_{\pm}/\mathrm{d}E$ against the period $T(E) = \mathrm{d}S/\mathrm{d}E \propto E^{-1/4}$ (broken curve); the exact densities do not diverge at $E = 0$ ($\Theta_+(0) = 2\Theta_-(0) = 2^{-5/3}3^{1/6}\pi^{-2}\Gamma(1/3)^5 \simeq 5.288318$), and their difference ($\Theta_+(E) - \Theta_-(E)$) accounts for the parity-dependent tunnelling level shifts discussed in [3].

In geometrical form, the system (2.2)–(2.3) is hardly less elementary than its harmonic-oscillator counterpart; but instead of being assigned a fully explicit value, each level E_k is kept locked in place by all its partners of the same parity. (This gives a new striking illustration of spectral rigidity: we can think of every single interval $[0, E_k]$ as being monitored from all the points E_ℓ at once through a mirror consisting of the half-line $\arg E = \pi/(M+1)$; self-monitoring has a null effect since $\theta_E[0, E] =$ constant.) A simple consequence is the quantization of every level spacing $[E_k, E_{k+2}]$ to exactly 4π in the coordinate $\Sigma_{\pm}$ of the corresponding parity. With the zero-point contributions properly counted, the resummed expressions of the divergent series $\Sigma^0(E)$ read as

$$\Sigma^{\pm}(E) = \Sigma_{\pm}(E) - [\pm\pi(M-1)/(M+1)]. \tag{2.4}$$

These resummed forms in no way supersede the original expansion (2.1). From equations (2.2)–(2.3) alone we can regenerate neither the levels nor even the semiclassical series (2.1), if only because the system (2.2)–(2.3) is totally insensitive to global rescalings of the spectrum. This system, in effect, constitutes a bootstrap or self-consistent loop essentially made of two mappings, one from charge distributions (on the rotated axis) to the induced fluxes $\Sigma(E)$ on the positive axis, given by equation (2.3) which naturally generates a linear map Φ, and a BS mapping $\mathcal{Q}$ which quantizes arclength functions $\Sigma(E)$ to discrete spectral staircases according to equation (1.2) and is basically nonlinear. The exact spectrum is a fixed point of the complete loop, i.e.

$$\begin{array}{ccc} \text{shifted arclength } \Sigma^{\pm}(E) & \xrightarrow{\quad\mathcal{Q}\quad} & \mathcal{N}_{\pm}(E) \text{ quantized spectrum} \\ \left(\text{subtract } \pm\pi\dfrac{(M-1)}{(M+1)}\right)\uparrow & & \downarrow\left(\text{rotate by } \dfrac{2\pi}{(M+1)}\right) \\ \text{induced flux function } \Sigma_{\pm}(E) & \xleftarrow[\quad\Phi\quad]{} & \text{distribution of charges } (+4). \end{array} \tag{2.5}$$

2.2. *Numerical application*

Our next result is that this bootstrap loop appears to converge numerically towards the exact eigenvalues by simple iteration, provided some scale constraint remains externally enforced. All operations will be understood within a given parity sector (selected beforehand).

In a first approach, we can restrict the computation to a finite energy interval, taking the arclength function $\Sigma_{\pm}(E)$ and levels E_k to be known everywhere else. This is the case in actual practice to any prescribed accuracy $\varepsilon > 0$: since the series (2.1) is asymptotic, some truncation of it numerically matches the function $\Sigma^{\pm}(E)$ above some eigenvalue E_{k_0}, for a suitably large $k_0(\varepsilon)$. These spectral data are then taken as exact and final, to be kept 'frozen' (as in an earlier non-iterative method using the trace identities to improve the lower eigenvalues [4]). Now, starting from a spectrum in which a trial value $E_k^{(0)}$ has been input for each lower level (i.e. $k < k_0$), we build the flux function generated by that complete spectrum (rotated); using this function we then requantize each lower level spacing to a flux value 4π downwards from E_{k_0}, getting a new sequence of lower levels $E_k^{(1)}$ as output (the alternative use of equation (2.2±) from $E = 0$ upwards works too); this whole elementary procedure can now be iterated. All our tests (with $M = 2$ or 3) then show a definite attraction of the lower levels towards their exact values, even from some quite distorted initial inputs (table 1). The convergence looks geometrical with a positive contraction factor which we denote $\kappa_{2M}^{\pm}(k_0)$. For the even spectrum of the quartic oscillator, for instance, $\kappa_4^{+}(k_0) \approx 0.3915 - 0.177/\sqrt{k_0}$ (from a numerical fit for $2 \ll k_0 \lesssim 160$).

The temptation is now to relax the above constraints and let $k_0 \to \infty$. Our subsequent analysis will, however, show that the limiting process has singular aspects. Nevertheless, we have evidence that a contractive behaviour can persist in the iteration of the full original loop (2.5), provided a correct asymptotic behaviour is enforced. For a numerical implementation, an admissible (say, relative) uncertainty ε must be prescribed to make the scheme finite. Now, the initial trial spectrum is only to satisfy the zeroth-order Bohr–Sommerfeld condition (1.1) asymptotically ($E \to +\infty$); this property is then preserved under the iteration. Hence, at each step, the newly computed arclength $\Sigma^{\pm}(E)$ and eigenvalues will numerically merge again (within ε) with their zeroth-order Bohr–Sommerfeld values at some energy E_{k_0}; any higher-energy calculations for that step can then be bypassed. A cutoff index k_0 is thus re-established, but now it is controlled by the iteration itself and by the value of ε. Table 2 demonstrates the power of that scheme in which only zeroth-order asymptotic information supplements the fixed-point equation (2.4).

Table 1. Lower part of the odd spectrum for the sextic potential q^6 ($M = 3$). This iteration uses the exact spectral data frozen from E_{11} upwards and arbitrarily initialized lower levels. The final values agree at the displayed accuracy with the actual eigenvalues (obtained by a matrix diagonalization for the lower end matched with a high-order WKB formula (2.1) from the upper end; cf also the values $2^{3/4}\epsilon_n$ from [5], table VI). The observed contraction factor is $\kappa_6^-(11) \approx 0.267$.

Step	E_1	E_3	E_5	E_7	E_9
0	5.000 000 000 0	5.000 000 000 0	5.000 000 000 0	5.000 000 000 0	5.000 000 000 0
1	3.277 108 414 0	8.855 860 265 5	21.517 638 492 4	41.090 373 619 1	63.805 086 141 1
2	3.992 898 866 6	13.857 554 669 1	28.220 206 944 5	45.835 311 929 3	66.015 951 322 0
5	4.333 092 303 4	14.927 644 034 9	29.293 414 869 1	46.591 093 313 0	66.385 320 497 1
10	4.338 591 576 1	14.935 161 204 2	29.299 639 481 9	46.595 207 351 1	66.387 279 799 3
15	4.338 598 702 0	14.935 169 623 7	29.299 645 928 8	46.595 211 443 1	66.387 281 704 1
$\geqslant 20$	4.338 598 711 5	14.935 169 634 9	29.299 645 937 4	46.595 211 448 5	66.387 281 706 6

Table 2. A few even eigenvalues of the quartic potential q^4 ($M = 2$). This iteration uses the zeroth-order Bohr–Sommerfeld condition (1.1) as the only additional dynamical constraint to be matched with the accuracy $\varepsilon = 10^{-8}$ (the resulting cutoff values k_0 are listed); the initial state is also the zeroth-order Bohr–Sommerfeld spectrum, except for the lowest two levels due to a most unfortunate mishandling. In spite of this, the correct eigenvalues [6, 2] ultimately emerge at the accuracy under display.

Step	k_0	E_0	E_2	E_4	E_8	E_{16}
0	3256	3.141 592 65	0.577 215 66	16.233 614 7	37.904 471 8	91.786 147 3
1	2736	0.725 277 07	6.732 902 44	15.679 924 8	37.553 624 7	91.591 0036
2	3954	0.903 944 90	7.257 168 84	16.073 340 6	37.761 258 6	91.673 5524
3	4212	0.995 152 19	7.382 243 89	16.193 463 7	37.861 317 0	91.745 2466
7	582	1.058 793 82	7.453 924 51	16.260 182 5	37.921 487 7	91.796 6881
14	1464	1.060 359 90	7.455 695 42	16.261 823 7	37.922 998 8	91.798 064 7
$\geqslant 21$	1466	1.060 362 09	7.455 697 93	16.261 826 0	37.923 001 0	91.798 066 8

Table 3. Observed orders of magnitude for the contracting factors of the bootstrap loop (2.5).

$V(q)$	q^4	q^6	q^8	q^{10}	q^{12}
Even	0.391–0.392	0.588–0.590	0.706–0.709	0.78–0.80	0.83–0.86
Odd	0.331–0.335	0.489–0.495	0.590–0.605	0.65–0.66	0.69–0.71

In comparison with the previous scheme, this one has a lower numerical efficiency (improvable by using first-order asymptotic information as input and/or a variable ε scaled down by stages). However, its number of degrees of freedom being *a priori* unbounded, it gives a better representation of the abstract, infinite-dimensional mapping (2.5). Table 3 lists a few contraction factors $\kappa_{2M}^{\pm}$ as estimated from this numerical approximation to the loop (2.5). These factors appear to be mainly influenced by the proximity of the lowest unfrozen eigenvalue (after rotation): thus, $\kappa_{2M}^{+} > \kappa_{2M}^{-}$, and in each parity class $\kappa_{2M}^{\pm}$ grows with M.

We can conclude from our numerical evidence that the bootstrap loop (2.5) drives many initial data that are only asymptotically correct towards the exact solutions, in a contractive manner. At present, we cannot ascertain that this property will persist for arbitrarily large M, especially in the even sector.

3. Preliminary analysis of the bootstrap loop

3.1. The flux operator

The mapping $\mathcal{N}_\pm(E) \longrightarrow \Sigma_\pm(E)$ defined by equation (2.3) can be expressed by a linear operator Φ, as

$$\Sigma_\pm(E) = \int_0^\infty 4\,\mathrm{Arctan}\frac{\sin(2\pi/(M+1))\,E}{E' - \cos(2\pi/(M+1))\,E}\,\mathrm{d}\mathcal{N}_\pm(E') = \int_0^\infty \frac{4\sin(2\pi/(M+1))\,E}{E'^2 - 2\cos(2\pi/(M+1))\,EE' + E^2}\mathcal{N}_\pm(E')\,\mathrm{d}E' \tag{3.1}$$

under the determination $0 \leqslant \mathrm{Arctan}\,z < \pi$. This operator commutes with dilations (it is a multiplicative convolution); hence it is diagonalized by a Mellin transformation. The most convenient one is that which maps the spectral functions $\mathcal{N}_\pm(E')$ into the standard (even/odd) spectral zeta functions, [4, 7]

$$Z^\pm(s) = \int_0^\infty E^{-s}\,\mathrm{d}\mathcal{N}_\pm(E) = \sum_{k\ \substack{\text{even}\\\text{odd}}} E_k^{-s} \qquad \frac{M+1}{2M} < \mathrm{Re}\,s \tag{3.2}$$

so we define flux zeta functions in the same manner:

$$\mathcal{Z}^\pm(s) = \int_0^\infty E^{-s}\,\mathrm{d}\Sigma_\pm(E) = s\int_0^\infty E^{-s-1}\Sigma_\pm(E)\,\mathrm{d}E \qquad \frac{M+1}{2M} < \mathrm{Re}\,s < 1 \tag{3.3}$$

the flux operator then acts as

$$\mathcal{Z}^\pm(s) = \widetilde{\Phi}(s)Z^\pm(s) \qquad \widetilde{\Phi}(s) = 4\pi\frac{\sin[(M-1)/(M+1)]\pi s}{\sin \pi s}. \tag{3.4}$$

3.2. The BS quantization mapping

We now pursue the same approach upon the mapping $\mathcal{Q} : \Sigma(E) \longrightarrow \mathcal{N}(E)$ defined by equations (1.2)–(1.3) (with $\hbar = 1$), and further decomposable as $\mathcal{Q}^+ + \mathcal{Q}^-$ (by splitting the sum over even and odd k). The induced mappings have the structure $\mathcal{Z}^\pm(s) = (1/4\pi)\mathcal{Z}(s) + \widetilde{\mathcal{Q}}^\pm_{\mathrm{osc}}\{\mathcal{Z}\}(s)$. The first term simply expresses the linear action of $\overline{\mathcal{Q}}^\pm$ ($= \mathrm{Id}/4\pi$), the second one is, however, quite intractable (nonlinear, non-local) except for its filtering action upon the singularities of $\mathcal{Z}^\pm(s)$: those (and only those) singular terms of $(1/4\pi)\mathcal{Z}(s)$ which arise (under the Mellin transformation) from the $E \to +\infty$ asymptotic behaviour of the input $\Sigma(E)$ turn up identically in $\mathcal{Z}^\pm(s)$, unaffected by $\widetilde{\mathcal{Q}}^\pm_{\mathrm{osc}}$ (as opposed to the other singularities, which encode the $E \to 0$ behaviour of $\Sigma_\pm(E)$: these are altogether suppressed in $\mathcal{Z}^\pm(s)$). More specifically, if the asymptotic input is supplied as

$$\Sigma(E) \underset{E\to+\infty}{\sim} \sum_{n=0}^{\infty} b_n E^{-i_n} \qquad \text{where } \{i_n\} \uparrow +\infty \tag{3.5}$$

then (provided all $i_n \neq 0$) $Z^\pm(s)$ is analytic for $\mathrm{Re}\,s > -i_0$ and, e.g., by Euler–Maclaurin continuation of equation (3.2) [7]

$$Z^\pm(s)/s \text{ has one simple pole at } s = -i_n, \text{ with residue } b_n/4\pi \qquad n = 0, 1, 2, \ldots \tag{3.6}$$

$$\text{and also at } s = 0, \text{ with residue } \pm 1/4 \qquad (\text{trace identity at } s = 0). \tag{3.7}$$

Equation (3.6) means that both mappings $\mathcal{Q}^\pm$ can be simplified to their common linear term $\overline{\mathcal{Q}}^\pm = \mathrm{Id}/4\pi$ as far as $E \to +\infty$ expansions, or the associated zeta-function singularities, are concerned.

3.3. The bootstrap loop in the Mellin picture

Awaiting a deeper analysis of the nonlinearities in the mappings $\mathcal{Q}^{\pm}$, we will mostly examine a linear problem: how $E \to +\infty$ asymptotic data behave under the bootstrap loop. We choose to enter the diagram (2.5) at the upper-left corner, with a formal $E \to +\infty$ expansion of the general form (common to both parities)

$$\Sigma^0(E) = \sum_{n=0}^{\infty} b_n E^{-i_n} \qquad i_n \text{ not integers} \qquad \{i_n\} \uparrow +\infty \qquad i_n > 0 \text{ except } i_0 < 0 \quad (3.8)$$

which is obeyed by the actual solution (2.1), in which case [7]

$$i_n = (2n-1)\frac{M+1}{2M} \qquad \text{(and: } b_n \equiv 0 \text{ whenever } i_n \text{ is integer).} \quad (3.9)$$

The action of $\mathcal{Q}^{\pm}$ thereupon amounts to multiplication by $1/4\pi$ as argued before. The subsequent action of the flux operator Φ is completely explicit in equation (3.4); from the analytic structure of the resulting $\mathcal{Z}^{\pm}(s)$ we then deduce, by inverting the second of the Mellin transforms (3.3), the asymptotic $E \to +\infty$ behaviour

$$\Sigma_{\pm}(E) \sim \sum_{n=0}^{\infty} \sigma_n E^{-i_n} + \mathcal{Z}^{\pm}(0) - 4\sum_{p=1}^{\infty}(-1)^p \frac{\sin[(M-1)/(M+1)]\pi p}{p} Z^{\pm}(-p)E^{-p}$$
$$\sigma_n = \frac{\sin[(M-1)/(M+1)]\pi i_n}{\sin \pi i_n} b_n \quad (3.10)$$

next, equations (3.4) and (3.7) yield

$$\mathcal{Z}^{\pm}(0) = \pm\pi(M-1)/(M+1) \quad (3.11)$$

causing the constant term in equation (3.10) to precisely cancel the anharmonic shift $\pm 2\pi C_M$ in equations (2.2) and (2.4). This coincidence is required by global consistency as it reduces the exact quantization conditions to

$$\mathcal{N}^{\pm}(E) = \mathcal{Q}^{\pm}\{\Sigma^{\pm}\}(E) \qquad \Sigma^{\pm}(E) = \Sigma_{\pm}(E) - \mathcal{Z}^{\pm}(0) \quad (3.12)$$

which indeed makes the loop close properly.

(Taking $\mathcal{Z}^{\pm}(0)$ from the analytically continued Mellin transforms (3.3), namely

$$\mathcal{Z}^{\pm}(s) = \int_0^{\infty} E^{-s}\, \mathrm{d}(\Sigma_{\pm}(E) - b_0 E^{-i_0}) \qquad -i_1 < \mathrm{Re}\, s < -i_0 \quad (3.13)$$

we identify the shifted functions $\Sigma^{\pm}(E)$ as natural regularizations of the divergent integrals $-\int_E^{\infty} \mathrm{d}\Sigma_{\pm}(E')$:

$$\Sigma^{\pm}(E) = -\int_E^{\infty} \mathrm{d}(\Sigma_{\pm}(E') - \sigma_0 E'^{-i_0}) + \sigma_0 E^{-i_0} \quad (3.14)$$

as such, they have the meaning of 'arclengths measured from $E = +\infty$' in the sense of symbolic integration [8], as opposed to $\Sigma_{\pm}(E)$ which are measured from $E = 0$, see figure 1.)

The fixed-point condition for the asymptotic data then relates the two expansions (3.8) and (3.10) by

$$\Sigma^{\pm}(E) \underset{E\to+\infty}{\sim} \Sigma^{0}(E) \qquad \text{to all orders in } E. \tag{3.15}$$

For non-integer i_n this means $\sigma_n \equiv b_n$ hence

$$\frac{\sin[(M-1)/(M+1)]\pi i_n}{\sin \pi i_n} = 1 \tag{3.16}$$

which yields precisely formula (3.9) for the allowed exponents i_n but leaves the coefficients b_n completely undetermined. For integer powers E^{-p} the conditions involve trace identities, which are certain relations fulfilled indeed by the actual values $Z^{\pm}(-p)$ [4, 7] but not by trial data, making the iteration of asymptotic data diverge. Nevertheless, the singular structure is preserved in the strip $\{-1 < \mathrm{Re}\, s < 1\}$, implying that Bohr–Sommerfeld asymptotics to zeroth (or first) order are preserved. In the Mellin picture, the linear fixed-point condition refers to the singular part of $Z^{\pm}(s)$ so that it reads as

$$Z^{\pm}(s) = \frac{\sin[(M-1)/(M+1)]\pi s}{\sin \pi s} Z^{\pm}(s) + A(s) \qquad (A(s) = \text{analytic function}). \tag{3.17}$$

The solution is obvious as is the fact that the corresponding iteration (Neumann series) is not globally contractive; it is especially divergent near the poles of $Z^{\pm}(s)$ (given by the condition (3.16)). Just as the semiclassical series refused to converge to this exact solution, the latter will not yield any of the coefficients b_n (the residues of $4\pi Z^{\pm}(s)/s$) through iteration; the two approaches thus do not overlap and can only communicate by analytical continuation (e.g., in s).

Still, the linear operator being iterated ($\widetilde{\Phi}(s)/4\pi$) is contractive somewhere: in the strip $\{-i_1 < \mathrm{Re}\, s < -i_0\}$, where the Mellin transforms (3.3) have the modified expression equation (3.13). Hence it is the spectral fluctuations (the deviations from zeroth-order Bohr–Sommerfeld, or Weyl, predictions) that are contracted towards zero. This is true for any reasonable norm defined within that s-variable strip, which includes many Sobolev-like norms (weighted, distributional, etc, in the $\log E$ variable) for the fluctuations; for a norm defined on the imaginary s-axis, the contraction factor is $\kappa_{2M}^{(0)} = (M-1)/(M+1)$. What remains to be rigorously proven is the intuitive idea that, as in the Euler–Maclaurin summation formula, the spectrum discretization step (for which the nonlinear maps $\mathcal{Q}^{\pm}$ replace $\overline{\mathcal{Q}}^{\pm}$) introduces but a small (contractivity-preserving) perturbation to this picture; the convergence must then simply be deflected towards the exact (instead of zeroth-order) results. We finally observe that, indeed, the contraction factors in table 3 are close to $\kappa_{2M}^{(0)}$, especially the odd ones!

4. Generalizations (on a speculative basis)

The exact Bohr–Sommerfeld conditions (2.2)–(2.3) were extracted from resurgence relations [9] and functional equations [1, 9] associated with homogeneous polynomial potentials. While resurgence formulae have a specially simple form for the monomials q^{2M}, they are also known for the general polynomial case [10, 11]. Put in integral form, very schematically they provide a set of integral equations for a system of analytic functions $\dot{a}_{ij}(x)$, where

$x \equiv \hbar^{-1}$, $\{ij\}$ expresses the indexing by all pairs of turning points (q_i, q_j) in the complex q-plane, and each pair is encircled by a cycle γ_{ij}:

$$\log \dot{a}_{ij}(x) = -x \oint_{\gamma_{ij}} p \, dq + \sum_{(q_k, q_l)} \Phi_{ij,kl}[\log(1 + \dot{a}_{kl}(x))]. \tag{4.1}$$

In this system, each $\widetilde{\Phi}_{ij,kl}(s) \propto \sin(\varphi_{ij,kl} s)/\sin \pi s$ which is like a flux operator ($|\varphi_{ij,kl}| < \pi$), whereas each mapping

$$x^{-1} \log \dot{a}_{kl}(x) \longrightarrow \log(1 + \dot{a}_{kl}(x)) \tag{4.2}$$

is analytically of the BS type (compare the Taylor expansion of the right-hand side with equation (1.3), identifying Σ with $i\hbar \log \dot{a}$). There should actually appear a different mapping $\mathcal{Q}_{kl}$ for each pair of turning points, i.e. one BS mapping attached to each harmonic oscillator qualifying as a local approximate comparison potential. Having thus identified abstract analogues of the ingredients used in equation (2.5), and recalling that contractive mappings have some stability under perturbation, we expect that bootstrap loops with properties similar to (2.5) can be extracted from structures like (4.1) corresponding to general polynomial potentials; they ought to be more elaborate, perhaps not unique, and possibly complex rather than real.

Further details and derivations will be given in a later publication.

References

[1] Sibuya Y 1975 *Global Theory of a Second-Order Linear Ordinary Differential Operator with a Polynomial Coefficient* (Amsterdam: North-Holland)

[2] Bender C M, Olaussen K and Wang P S 1977 *Phys. Rev.* D **16** 1740–8

[3] Balian R, Parisi G and Voros A 1978 *Phys. Rev. Lett.* **41** 1141–4
Albeverio S *et al* 1979 *Feynman Path Integrals (Proceedings, Marseille, 1978) (Springer Lecture Notes in Physics 106)* ed S Albeverio *et al* (Berlin: Springer) pp 337–60

[4] Parisi G 1982 *The Riemann Problem, Complete Integrability and Arithmetic Applications (Springer Lecture Notes in Mathematics 925)* ed D Chudnovsky and G Chudnovsky (Berlin: Springer) pp 178–83

[5] Hioe F T, MacMillen D and Montroll E W 1976 *J. Math. Phys.* **17** 1320–37

[6] Reid C E 1970 *J. Mol. Spectrosc.* **36** 183–91

[7] Voros A 1982 *The Riemann Problem, Complete Integrability and Arithmetic Applications (Springer Lecture Notes in Mathematics 925)* ed D Chudnovsky and G Chudnovsky (Berlin: Springer) pp 184–208 (augmented version of: 1980 *Nucl. Phys.* B **165** 209–36) (Hint: $Z^{\pm}(s)$ (here) $\equiv C_M^{-(2M/(M+1))s}(Z(s) \pm Z^{P}(s))/2$ (in [7]).)

[8] Voros A 1987 *Commun. Math. Phys.* **110** 439–65

[9] Voros A 1982 *J. Physique Lett.* **43** L1–L4; 1992 *Zeta Functions in Geometry (Advanced Studies in Pure Mathematics 21) (Proceedings, Tokyo, 1990)* ed N Kurokawa and T Sunada (Kinokuniya: Mathematical Society of Japan) pp 327–58

[10] Ecalle J 1984 Cinq Applications des Fonctions Résurgentes *Preprint* Orsay Math. 84T62 unpublished

[11] Delabaere E, Dillinger H and Pham F 1993 *Ann. Inst. Fourier* **43** 163–99